inter-noise 2002

The 2002 International Congress and Exposition on Noise Control Engineering
Dearborn, MI, USA. August 19-21, 2002

Frequency Domain Analysis of Rattle in Gear Pairs and Clutches

T. C. Kim and R. Singh
Acoustics and Dynamics Laboratory
Department of Mechanical Engineering and Center for Automotive Research
The Ohio State University
Columbus, Ohio 43210-1107, USA

Abstract

In order to truly understand rattle noise and vibration sources in vehicle drivetrains, a torsional system model with one or more clearance non-linearities must be developed. Most prior analyses have focused on the determination of time domain responses under harmonic excitations using cumbersome numerical tools. In this paper, we propose an alternative prediction scheme that examines the nonlinear frequency response characteristics. We present a new semi-analytical scheme, based on the multi-term harmonic balance method (HBM). It is applied to the flywheel-clutch (with multi-staged stiffnesses), clutch hub-spline (with backlash) and gear pair (with backlash) sub-systems. Unlike the previous methods, our method includes parametric continuation with self-adjustable frequency steps, and it is capable of efficiently finding both stable and unstable solutions in multi-valued regimes. Calculated results are successfully compared with experimental data and numerical simulations. This versatile method could be used to develop design criteria for a rattle-free system.

1. Introduction

Rattle noise sources arise from gaps and multi-valued stiffness elements in a wide variety of machinery, vehicle and industrial applications. In this article, we focus on the torsional vibrations of a typical vehicle drivetrain that consists of many gear pairs with backlashes and a clutch with two or more stages in terms of its torque vs. relative angular displacement characteristics. Further, non-linear damping mechanisms are often present. To better understand this problem, consider the source-path-receiver network of Figure 1 where the sound pressure from the rattle sources, at a given engine speed Ω_p, can be defined as follows.

$$p(\Omega_p) = \sum_{i,j,k} \left(\frac{p}{a}(\Omega_p) \right)_i \left(\frac{a}{\ddot{q}}(\Omega_p) \right)_{j,k} \ddot{q}_j(\Omega_p) = \sum_{i,j,k} \left(\frac{p}{\ddot{q}} \right)_{i,j} \ddot{q}_j(\Omega_p)_k \tag{1}$$

Here, p is the pressure (at an interior or at the pass-by location), a is the structural acceleration of drivetrain housing, i denotes the path from housing vibration to p location,

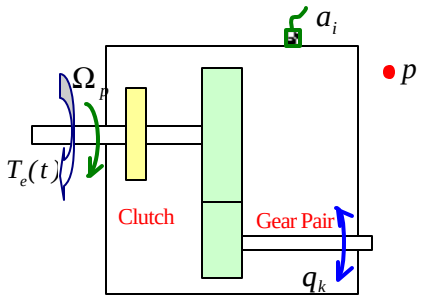

Figure 1. Schematic of a vehicle drivetrain with rattle sources.

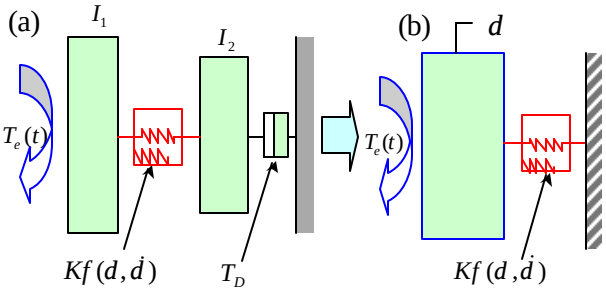

Figure 2. Torsional sub-system with clearance non-linearity. (a) 2DOF semi-definite system; (b) SDOF definite system.

index j is the path for torsional structure-borne noise, and $\ddot{q}_j$ is the torsional acceleration of the k^{th} rattle source. In this analysis, multiple paths could be quantified using linear experimental or computational methods. However, the knowledge of sources must be obtained by using a non-linear differential equation solver. Note that here p and $\ddot{q}$ are defined at a given speed and thus one must keep track of all periodic and non-periodic solutions. To illustrate the nature of this problem, examine the two degree of freedom (2DOF) torsional sub-system of Figure 2 that could be reduced to a single degree of freedom (SDOF) definite system in terms of relative angular displacement $d(t)$. Figure 3 shows a generic form of the clearance type non-linearity that induces rattle. Here the stiffness of the first stage is a with respect to the second stage of unity stiffness. The backlash problem is given when $a = 0$ and $-b$ to b regime will be equal to the amount of backlash. When $a \to \infty$ and $b = 0$, one find the typical characteristics of a torque converter clutch in a vehicle with automatic transmission. Finally, the clutch corresponding to a manual transmission is given by $0 < a < 1$.

Non-linear dynamics of a torsional system with one or more clearance non-linearities has been studied using digital [1, 2] and analog [3] simulation methods. However, such analyses emphasize the determination of response time history at a given harmonic excitation, and these require substantial computational resources. The resulting time history can be very complicated and may include super-harmonic and sub-harmonic resonances [1-4], or even chaotic motions [1-3]. Such a complex behavior prevents an engineer from efficiently judging the overall system response. Moreover, one must often run too many cases to find parameters that could avoid or reduce rattle. Therefore, from the design point of view, steady state frequency (speed) response functions of the governing system are needed. Nonetheless, the concept of a frequency response function is more complicated for the non-linear case, as it must include sub- and super-harmonics, multi-valued responses of a single frequency excitation, and jump phenomenon. One must also consider the possibility of non-periodic and chaotic solutions [1-3]. In this paper, we present a new semi-analytical method that can efficiently calculate the relevant frequency and time domain characteristics of a rattle source.

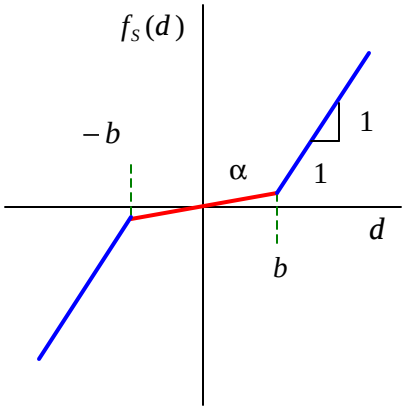

Figure 3. Torque-displacement characteristics of clearance type non-linearity.

2. New Solution Method

Assume that the rattle source can be well represented by a lumped model of Figures 2 and 3. The excitation torque $T_e(t)$, from an internal combustion engine, fluctuates significantly between low (around the compression stage) and high (around the ignition stage) values. Therefore, decompose $T_e(t)$ into mean T_m and perturbation $T_p(t)$ parts. The fundamental harmonic Ω_p of $T_p(t)$ depends on type of the engine, number of cylinders and crankshaft configuration. Express $T_e(t)$ via a Fourier series (with N harmonics) as shown below where j_n is the phase angle at the nth harmonic.

$$T_e(t) = T_m + \sum_{n=1}^{N} T_{pn} \sin(n\Omega_p t + j_n) \text{ or } T_e(t) = T_m + \sum_{n=1}^{N} T_{pn} \cos(n\Omega_p t + j_n) \tag{2}$$

The mean $T_m = \langle T_e(t) \rangle_t$ term, under "no power" condition, should be equal to the drag torque $T_D(\Omega_p, \Lambda)$ generated within the transmission where Λ is the gearbox temperature. After an application of the initial conditions in terms of absolute angular displacements, $\ddot{q}_1(0) = \ddot{q}_2(0) = 0$, and $q_2(0) = 0$, the relationship between T_D and T_m for Figure 2 is written as $T_D = I_2 T_m / I_1$. Therefore, the coupled non-linear second order differential equations for the semi-definite sub-system of Figure 1a are reduced to a single equation for the equivalent SDOF system of Figure 1b where $d = q_1 - q_2$.

$$\ddot{d} + \frac{C}{I}\dot{d} + \frac{K}{I} f(d, \dot{d}) = F(t) = F_m + \sum_{n=1}^{N} F_{pn} \sin(n\Omega_p t + j_n) \tag{3}$$

Here, C is the viscous damping coefficient, K is the linear stiffness corresponding to the second stage of the unity slope in Figure 2a, $I = I_1 I_2 / (I_1 + I_2)$ is the effective inertia, $F_m = T_m / I_1 + T_m / I_2$ is the effective external mean torque, and $F_{pn} = T_{pn} / I_1$ is the effective external pulsating torque at the nth harmonic.

Next, we propose a new multi-term harmonic balance method (HBM). It is essentially a form of the Galerkin's method based on the least squares fit in error reduction [5]. The residual or error $r(t)$ is the gap between true input and estimated solutions, and it should goes to zero for $d(t)$ that satisfies the non-linear differential equation. In time domain analysis, the residual should be zero for all time spans. This is called as the "strong" form since the satisfaction of time span requires an extensive calculation. From equation (3), before normalization by the inertia term I, the equation of motion becomes as below. The "strong" form residual is:

$$r(t) = T(t) - I\ddot{d} - C\dot{d} - Kf(d, \dot{d}) \to 0 \forall t. \tag{4}$$

However, when the input and response characteristics of a non-linear system are periodic, frequency domain analysis can be applied by introducing the Fourier transformation ($\Im$) of both sides. The Fourier transformation of equation (4) yields the following "weak" form residual.

$$\Im(r(t)) = \Im(T(t)) - I\Im(\ddot{d}) - C\Im(\dot{d}) - K\Im(f(d, \dot{d})) \tag{5}$$

Let the Fourier component vector of the sampled output be $\underline{a} = \Im(d(t))$, then the minimization of the residual in Newton-Raphson form is expressed as $R \cong R_0 + (\partial R / \partial \underline{a}) \Delta \underline{a}$. Here, R_0 is the residual from an initial guess, and the correction factor is defined as $\Delta \underline{a} = -(\partial R / \partial \underline{a})^{-1} R$. Finding a true $\underline{a}$ is an iterative process, and the Newton-Raphson

scheme is used. The term $\partial R / \partial \underline{a}$ is the Jacobian matrix $\underline{\underline{J}}$ used in the Newton-Raphson corrector and finding $\partial \underline{c} / \partial \underline{a}$ in $\underline{\underline{J}}$ is the key of HBM. The term $\partial \underline{c} / \partial \underline{a}$ is strictly related to non-linearity in the sub-system and defined as below.

$$\frac{\partial \underline{c}}{\partial \underline{a}} = \frac{\partial (\underline{\underline{\Gamma}}^* \underline{f})}{\partial \underline{a}} = \underline{\underline{\Gamma}}^* \frac{\partial \underline{f}}{\partial \underline{a}} = \underline{\underline{\Gamma}}^* \frac{\partial \underline{f}}{\partial \underline{\delta}} \frac{\partial \underline{\delta}}{\partial \underline{a}} = \underline{\underline{\Gamma}}^* \frac{\partial \underline{f}}{\partial \underline{\delta}} \underline{\underline{\Gamma}} \tag{6}$$

The critical term below is the instantaneous stiffness of non-linear function $f(d)$ at each sampling points.

$$\frac{\partial \underline{f}}{\partial \underline{\delta}} = \underline{\underline{f_\delta}} = diag\left(\frac{\partial f}{\partial \delta}(t_0) \quad \frac{\partial f}{\partial \delta}(t_1) \quad \cdots \quad \frac{\partial f}{\partial \delta}(t_{N-1}) \quad \frac{\partial f}{\partial \delta}(t_N) \right) \tag{7}$$

Additionally, an arc-length continuation scheme [5] is implemented in HBM by introducing an independent scalar parameter w, which is the excitation frequency over the rage of frequency-domain analysis. Refinement of the arc-length can be related to both numbers of iterations before convergence and changes in tangential angles of the frequency response function, and it greatly improves the convergence of the algorithm. With minimal computational cost, dynamic stability can also be analyzed in the frequency-domain by HBM.

3. Results and Discussion

To demonstrate the validity of HBM, an experimental system [4] is modeled. Numerical simulations (NS) based on a Runge-Kutta scheme are also run and their predictions are compared with those from HBM and measurements. As seen in Table 1, experimental and simulation results match exactly in peak-to-peak amplitudes. After a close examination of response curves in time domain, it is found that both simulation schemes yield the same time signatures as the experiment even in the non-linear stiffness transition regimes. For the numerical simulation, two runs, down and up frequency sweeps, are needed in order to achieve solution points around the non-linear resonance peak. This is because the numerical simulation tends to follow the stable results, and can only provide a single value in a multi-valued solution regime; this results in the jump phenomenon. This limitation can also be observed in non-linear experimental result. However, our HBM with parametric continuation capability adjusts itself for better convergence using Newton-Raphson type solutions, and calculates periodic solutions in multi-valued regimes. A single run of HBM can provide all results even in multi-valued regimes and the super harmonic peaks of $(1/n)\Omega_p$ with the same accuracy as numerical simulation in less than 1/10 of calculation time, as evident from Table 1.

Figure 4 shows a comparison between linear and non-linear frequency responses as calculated by HBM using the operating conditions of Table 2 for the sub-system of Figure 2 and 3. Here, d_m is the operating (mean) point around which dynamic perturbation takes place. The non-linear frequency response is generated by plotting d_{rms} vs. $\overline{\Omega}$ where $\overline{\Omega}$ is the dimensionless frequency (speed) and d_{rms} is the root-mean-square displacement. Corresponding to a harmonic excitation at Ω_p, one could run the numerical simulation and determine the steady state response. Then we can calculate the *rms* value of $d(t)$ that may include sub- or super-harmonics. The HBM yields this answer quickly unlike the numerical simulation.

The non-linear frequency response clearly demonstrates an amplitude sensitivity leading to severe rattle noise. The fundamental harmonic peak starts from the no-impact case with

$\overline{\Omega} = 1.00$, then reduces to $\overline{\Omega} = 0.65$ when it gets into single-sided impacts, and finally saturates to $\overline{\Omega} = 0.80$ for double-sided impacts. In addition, the non-linear frequency response exhibits several active super-harmonic responses below $\overline{\Omega} = 0.40$, and a sub-harmonic response above $\overline{\Omega} = 1.20$. The linear frequency response curve can not obviously predict these phenomena and their amplitudes are lower than those from non-linear analysis. For example, there would at least a 20 dB difference in sound pressures generated by a rattle source between the linear and non-linear simulations, around $0.6 < \overline{\Omega} < 0.8$.

Table 1: Comparison of simulation and experiment

	Experiment	NS	HBM
$\lvert\ddot{\theta}\rvert$ (rad/s^2), p-p	410	409	409
Computation Time (T)	-	3,640 s	350 s

Table 2: Operating condition of the sub-system of Figures 2 and 3

d_m starts from the 2nd stage stiffness	Impact Case	$K = 1.0$, $I = 1.0$, $C = 0.05$, $a = 0.25$
	Double-sided	$F_m = 0.050$, $F_{p1} = 0.030$, $b = 0.000$, $b = 10°$

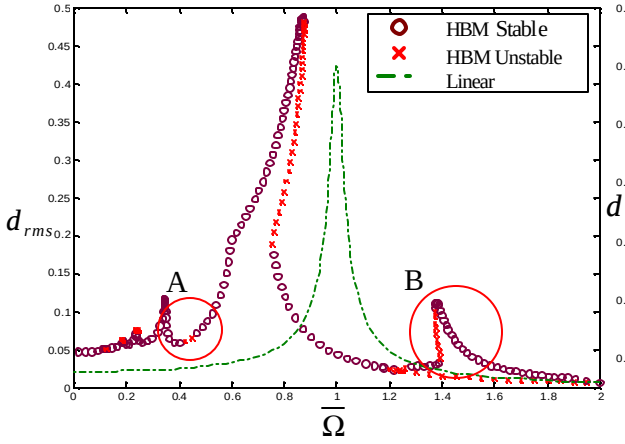

Figure 4. Comparison between linear and non-linear frequency responses.

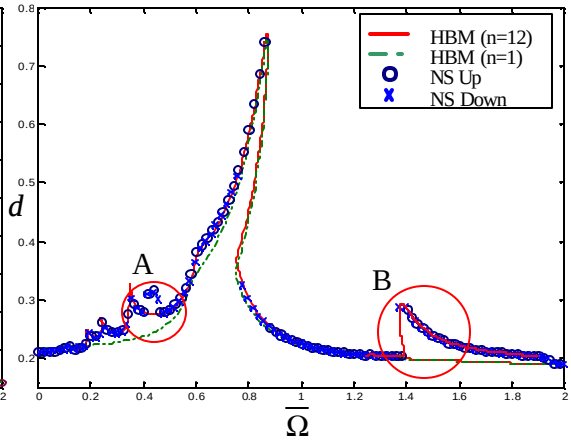

Figure 5. Comparison between numerical simulation and HBM.

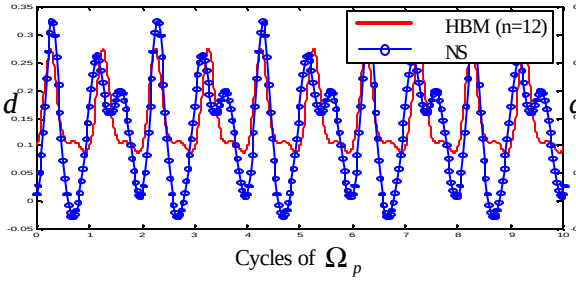

Figure 6. Time history of quasi-periodic response ("A" at $\overline{\Omega} = 0.44$).

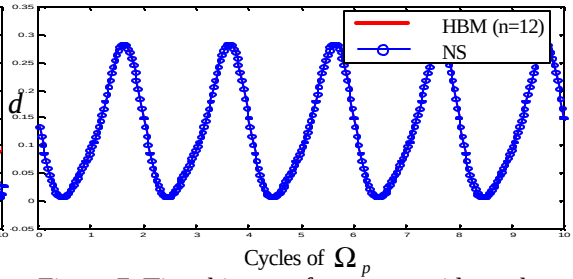

Figure 7. Time history of response with a sub-harmonic ("B" at $\overline{\Omega} = 1.41$).

Furthermore, the stability indicator in our HBM shows the possible appearances of chaotic or quasi-periodic ("A"), and sub-harmonic ("B") regimes. As noted in Figures 4 and 5, there is a small regime ("A") where the HBM and numerical simulation results do not match well. From the numerical simulation, this is a quasi-periodic regime as shown in Figure 6. Since

HBM is assumed to have only periodic solutions, chaotic and quasi-periodic or aperiodic responses could result in unstable solutions. As seen in Figure 6, the period is doubled in the numerical simulation when compared to the periodic HBM solution. Yet, another instability occurs in the sub-harmonic regime ("B"). Even though sub-harmonic responses are periodic, they are unstable in terms of the assumed Ω_p solution. Re-running HBM with $n\Omega_p$ can simulate the nth sub-harmonic resonances. The HBM assumes the periodic solution but with a frequency $2\Omega_p$. It results in a sub-harmonic peak at $\overline{\Omega} = 1.4$, as evident from the time domain signature in Figure 7. Numerical simulation and HBM results match exactly since sub-harmonic response is still periodic. The mean operating point d_m migrates back and forth from the second stage of the stiffness to the first stage (Figure 3) during the frequency sweep. An appearance by the sub-harmonic resonance depends upon the $\overline{\Omega}$ separation between the primary harmonic and mean operating point crossover point. When the separation in $\overline{\Omega}$ is greater than the primary harmonic resonance frequency ($\overline{\Omega}_1 = 0.65$ in Figure 4), then a sub-harmonic resonance peak would appear around $\overline{\Omega} = 1.4$.

4. Conclusion

The HBM can be used to generate new insights about the rattle sources and thus develop useful design guidelines. For example, when designing a gear pair or a clutch, response maps of Figure 5 and the like can be used to avoid possible vibro-impacts. In the case of a clutch, the range given by $0.10 < \alpha < 0.30$ and $0.3 < \overline{\Omega} < 3.0$ should be avoided. This is because super- and sub-harmonics as well as quasi-periodic responses, as shown in Figure 5, are found there. The response maps need to be constructed according to each a value, given certain mean and alternating torque conditions. Our semi-analytical method (HBM) with parametric continuation and stability analysis can effectively predict the non-linear frequency (speed) response of a torsional rattle system even in the presence quasi-periodic, chaotic and sub-harmonic regimes. Furthermore, the response maps developed by the HBM provide important clues and suggestions that could lead to the avoidance or reduction of vibro-impacts. Finally, ongoing research work is examining non-linear damping mechanisms.

Acknowledgements

This project has been supported by the Gear Rattle Industrial Consortium (Eaton R & D, Spicer Clutch, CRF Fiat, Luk, SAAB and Volvo Trucks over the 1998-2000 period), and DaimlerChrysler Challenge Fund since 2000. Personal discussions with T. E. Rook in developing the HBM code are gratefully acknowledged.

References

1. R. SINGH, H. XIE and R. J. COMPARIN 1989 *Journal of Sound and Vibration* **131**, 177-196. Analysis of an automotive neutral gear rattle.
2. R. J. COMPARIN and R. SINGH 1989 *Journal of Sound and Vibration* **134**(2), 259-290. Non-linear frequency response characteristics of an impact pair.
3. R. J. COMPARIN and R. SINGH 1990 *Journal of Sound and Vibration* **142**, 101-124. Frequency response of multi-degree of freedom system with clearances.
4. C. PADMANABHAN, R. C. BARLOW, T. E. ROOK, and R. SINGH 1995 *Journal of Mechanical Design* **117**, 185-192. Computational issues associated with gear rattle analysis.
5. G. VON GROLL and D. J. EWINS 2001 *Journal of Sound and Vibration* **241**(2), 223-233. The Harmonic Balance Method with Arc-Length Continuation in Rotor/Stator Contact Problems.